

Transient Thermal Analysis using both Lumped-Circuit Approach and Finite Element Method of a Permanent Magnet Traction Motor

Y.K. Chin, D.A. Staton

Abstract – This paper presents the transient thermal analysis of a permanent magnet (PM) synchronous traction motor. The motor has magnets inset into the surface of the rotor to give a maximum field-weakening range of between 2 and 2.5. Both analytically based lumped circuit and numerical finite element methods have been used to simulate the motor. A comparison of the two methods is made showing the advantages and disadvantages of each. Simulation results are compared with practical measurements.

Index Terms – Thermal Analysis, Lumped-circuit, Finite Element Method, Permanent Magnet Synchronous Motor

I. INTRODUCTION

Heat transfer is the science that seeks to predict the energy transfer that takes place between material bodies as a result of a temperature difference. When designing an electric motor, the study of heat transfer is as important as electromagnetic and mechanical design. However, due to its three dimensional nature, it is generally considered to be more difficult than the prediction of the electromagnetic behaviour [1]. For this reason, and the fact that the majority of designers have an electrical rather than mechanical background, thermal analysis is usually not given as much emphasis as the electromagnetic design. Owing to the continuing improvements in computation capability and improvements in thermal design software it is now possible to calculate the thermal performance with relative ease and good accuracy. Thus, there is now no excuse not to thoroughly analyse the motor thermally. In doing so the designer can gain large improvements in the overall design that would not be possible by optimising the electromagnetic design alone.

A comprehensive thermal model gives the user a clear understanding of the important thermal aspects of a design and which criteria the design is most sensitive to, i.e. interface resistances, winding impregnation, air flow, radiation, etc. With this information the designer can make informed decisions when looking at optimising the design, especially when compromises must be made, e.g. more and/or larger fins or an improved impregnation system will add cost and may not give a large improvement in cooling.

There are many difficult areas of thermal analysis that depend on the manufacturing methods, manufacturing tolerances and the materials used. An example is the contact resistance between components in the motors construction. The interface between the housing and stator lamination is

very dependent upon the manufacturing methods used to prepare the surfaces and the method used to insert the stator into the housing. Also, an aluminium housing should have a lower interface thermal resistance than a cast iron housing due to its relative softness. However, its increased thermal expansion at high temperatures can eliminate this advantage. Other examples of where the thermal model is dependent on such factors are the winding thermal model (in particular its impregnation), bearing heat transfer, forced convection cooling of open fin channels with shaft mounted fans. Empirical data is available to help the designer set realistic values for such parameters [2]. More accurate results can usually be found if the designer carries out their own testing and calibrates the models used.

This study presents the thermal analysis of a permanent magnet (PM) synchronous traction motor, using both analytical lumped circuit and numerical finite element methods. Section II gives details of the prototype motor studied (as shown in Fig. 1) and the load cycles concerned. Section III gives fundamental theory on the different heat transfer mechanisms commonly found in electric motors. Section IV describes the lumped-circuit analysis program, Motor-CAD [3], used in this work. The finite element analysis (FEA or FEM) packages, FEMLAB [4] and FLUX [5], are discussed in section V. Practical measurements carried out with the data are presented in section VI. Section VII compares the simulation results with the practical measurements. Conclusions are drawn in section VIII.

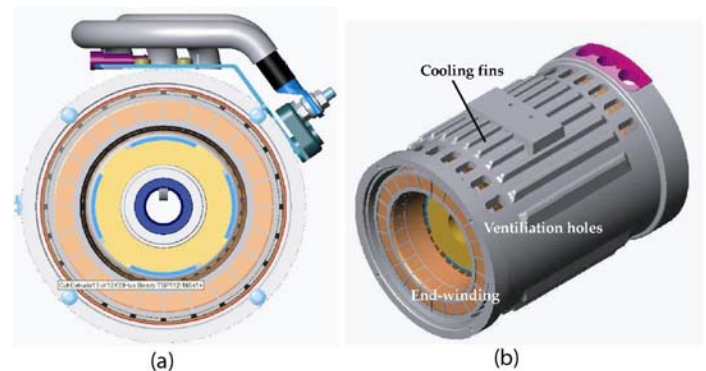


Fig. 1. The inset permanent magnet prototype motor studied. (a) Cross sectional view; (b) CAD drawing showing housing, end winding and cooling fins.

II. PROTOTYPE MOTOR

The prototype is a PM synchronous motor with magnets inset into the surface of the rotor as illustrated in Fig. 1(a). The magnets used are parallel-magnetised Samarium Cobalt (SmCo) VACOMAX 145S [6]. The active length and stator outer diameter are 165mm and 188mm respectively. It has a continuous power of 3.2kW and an operating speed up to 3900rpm when field-weakened. The motor's outer surface is naturally cooled. The housing has axial cooling fins as shown in Fig. 1(b), but these are only small and only give a marginal increase in cooling over a smooth housing. Axial fins are more suitable for a blown over cooling strategy such as TEFC. The cooled designation according to IEC 34 [7] is IC-01 as there are ventilation holes in the frame. However, in this case there is no internal fan on the shaft so the added cooling over a TENV machine is limited. Class F insulation is used.

In many applications the motor does not run continuously, but has an intermittent load. This is common in traction motors as studied here. Typically a fast acceleration is required to reach the maximum speed. It may operate at that speed for a short period and then decelerate to standstill (Fig 3(a)). Three standard IEC 34-1 [7] duty cycles, as shown in Fig 2 (S1, S2 and S3), are used in the prototype measurements. They are described below:

A. S1- Continuous operation

The motor is operating at a constant output power over an extensive period of time till the thermal steady state is reached. Thermal steady state or equilibrium is reached when the increase in temperature is less or equal than 1 degree Celsius over a period of one hour.

B. S2 – Short time operation

The motor is running at a constant power over a period that is shorter than that required to reach the thermal equilibrium. An off period then follows until the motor reaches ambient.

C. S3 – Intermittent operation

The motor is running with repeated cycles consisting of a constant output power period followed by an off period. The constant power period as a percentage of the time period is defined as the intermittent factor.

III. HEAT TRANSFER

In the following, conduction, convection and radiation heat transfer as found in the electrical machines are described:

A. Conduction

Conduction takes place due to vibration of molecules in a material. It is the heat transfer mechanism found in a solid body. It also occurs in liquids and gases, but convection is usually dominant here. Heat is transferred from a high-temperature region to a low-temperature region and is proportional to the temperature gradient:

$$q = -kA \frac{\partial T}{\partial x} \quad (1)$$

where q is the heat transfer rate, $\partial T/\partial x$ is the temperature gradient in the direction of the heat flow and k is the thermal conductivity of the material.

The thermal conductivity can be as low as 0.1 W/m°C for insulating materials and as high as 400 W/m°C for copper. Air has a value of 0.026 W/m°C at ambient temperatures and increases with temperature. Silicon iron has a thermal conductivity of between 20-55 W/m°C and is larger for high loss low silicon materials [2]. Aluminium alloy has a thermal conductivity around 170 W/m°C which is larger than the 52 W/m°C for cast iron. The thermal conductivity is more temperature dependent for some materials than others. Sometimes it is quite difficult to obtain reliable thermal conductivity data for materials used in the motors construction. This can be due to inadequate material data sheets or the fact that there may be air pockets leading to higher effective thermal conductivities than the pure material, i.e. non perfect impregnation. Sensitivity analysis can be used to vary the effective thermal conductivity between expected lower and upper bounds and to see the effect on the temperature rise. This is far easier to do using lumped circuit analysis due to the fast calculation speed and the fact that only one parameter need be varied. In fact this type of analysis can easily be automated and run from Excel or Matlab [8]

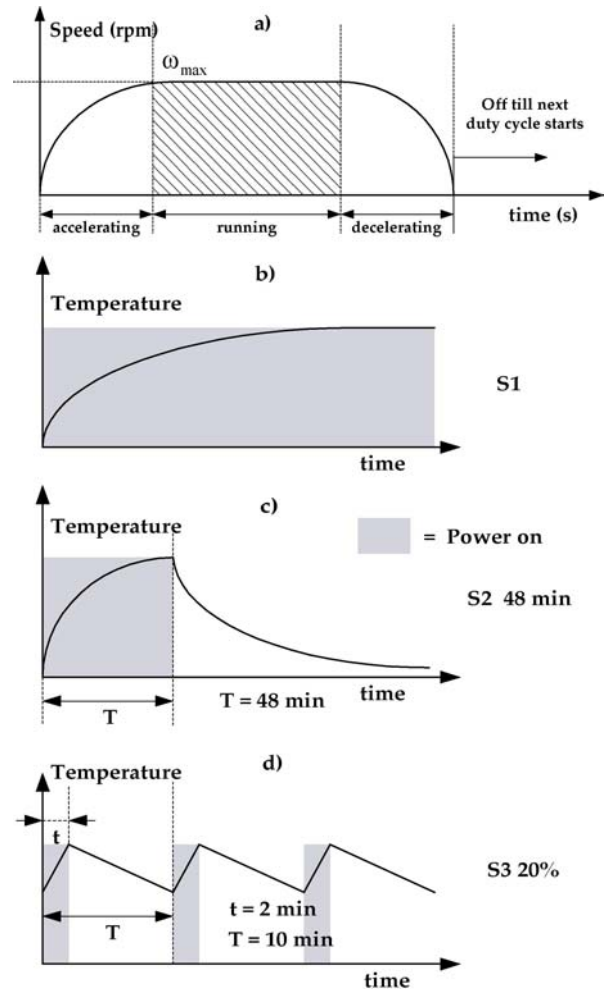


Fig. 2. a) Intermittent drive cycle; b) S1 – Continuous operation; c) S2 x min – Intermittent operation; c) S3 y% - Intermittent operation.

B. Convection

Convective heat exchange takes place between a hot surface and a fluid. The added heat transfer over pure conduction to the fluid is due to intermingling of the fluid immediately adjacent to the surface (at which point heat transfer is by conduction) with the remainder of the fluid. The fluid motion that gives rise to intermingling can be due to an external force (fan) and is termed forced convection. Alternatively it may be due to buoyancy forces and is termed natural convection. Convection heat transfer can be expressed using Newton's Law:

$$q_{conv} = hA(T_w - T_\infty) \quad (2)$$

h is the convection heat transfer coefficient, A is the surface area, T_w and T_∞ are the surface and fluid temperature respectively.

In electric machines common areas where the forced convection takes place are on the outer surface of the frame in a TEFC machine and in the internal air path of a through ventilated machine. In our case the areas where forced convection takes place is limited to the airgap and around the end-winding. Also, there is no internal fan so that the added air circulation over that of natural convection is limited.

The key to obtaining an accurate thermal model is to use proven empirical formulations (correlations) to gain an accurate value for the h coefficient for any convection surface in the machine. Heat transfer books such as [9] give many well used correlations for natural and forced convection from all types of surfaces found in electrical machines, i.e. flat plates, cylinders, fin channels, etc. Such correlations are based on empirical dimensionless analysis. The following dimensionless numbers are used: Reynolds (Re), Grashof (Gr), Prandtl (Pr) and Nusselt (Nu). For natural convection the typical form of the correlation is:

$$Nu = a (Gr Pr)^b \quad (3)$$

For forced convection the typical form is:

$$Nu = a (Re)^b (Pr)^c \quad (4)$$

where a , b and c are constants given in the correlation. Also:

$$Re = \rho v L / \mu \quad (5)$$

$$Gr = \beta g \Delta T \rho^2 L^3 / \mu^2 \quad (6)$$

$$Pr = c_p \mu / k \quad (7)$$

$$Nu = h L / k \quad (8)$$

- h - heat transfer coefficient [W/m²/°C]
- μ - fluid dynamic viscosity [kg/s.m]
- ρ - fluid density [kg/m³]
- k - fluid thermal conductivity [W/m/°C]
- c_p - fluid specific heat capacity [kJ/kg/°C]

- v - fluid velocity [m/s]
- ΔT - delta temperature of surface-fluid [°C]
- L - characteristic length of the surface [m]
- β - coef cubic expansion $1/(273 + T_{FLUID})$ [1/°C]
- g - gravitational force of attraction [m/s²]

The magnitude of Reynolds number (Re) is used to judge if there is laminar or turbulent flow in a forced convection system. Similarly the product of Gr and Pr is used in natural convection systems. Turbulent flows give enhanced heat transfer but added resistance to flow.

A well known correlation for predicting the heat transfer from concentric rotating cylinders [11] can be applied to the airgap heat transfer. Cooling of surfaces within the endcap region is slightly more difficult due to the complex flow patterns encountered [1,2]. There has been much research on this type of cooling and several correlations of the form given in equation (9) have been published:

$$h = k_1 \cdot (1 + k_2 v)^{k_3} \quad (9)$$

k_1 , k_2 and k_3 are the empirical constants and v is the velocity. Fig. 3 shows the variations of h with respect to the velocity [11-15] for the published correlations.

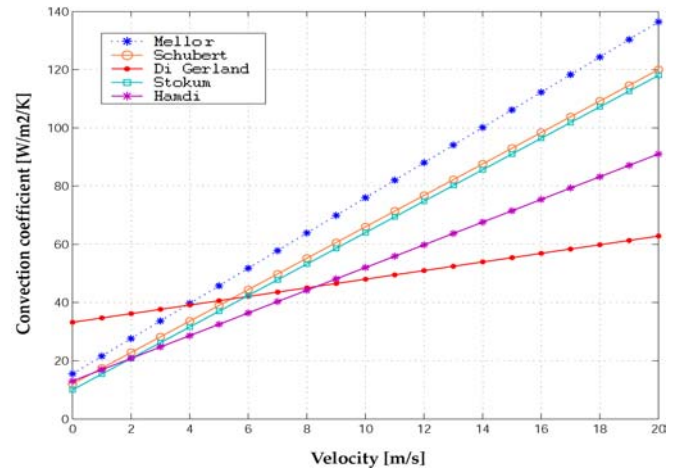


Fig. 3. Convection heat transfer coefficient versus air velocity for surfaces within the motor endcaps.

C. Radiation

Radiation is the heat transfer mode from a surface due to energy transfer by electromagnetic waves. It takes place in a vacuum and is proportional to the difference in absolute temperatures to the fourth power and the surface area:

$$q_{rad} = \epsilon_1 \sigma A \cdot (T_w^4 - T_\infty^4) \quad (10)$$

σ is the Stefan-Boltzmann constant and ϵ is the emissivity. Materials with different surfaces present different emissivities. For instance, a painted or dull aluminium housing can facilitate higher radiation compared to the original shiny housing.

IV. ANALYTICAL LUMPED CIRCUIT MODEL

A good way to gain a better understanding of thermal problems is to use the analogy between thermal and electrical networks. In the steady state the thermal network consist of thermal resistances and heat (power) sources connected to give a realistic representation of the main heat transfer paths and loss sources within the machine. The temperature (rather than voltage) at various nodes can be calculated together with the power (rather than current) flow between nodes. For transient analysis, thermal capacitances (rather than electrical capacitances) are added to account the change internal energy of the body with time.

The thermal resistances are derived from geometric dimensions, thermal properties of the materials and heat transfer coefficients. The thermal resistance for a conducting path can be calculated using the formulation:

$$R = \frac{l}{kA} \quad (11)$$

where l and A are the path length and areas respectively. This formulation lends itself to the analytical lumped circuit type of calculation as it is quite easy to identify a components effective length and area from its geometric shape. The thermal conductivity is just a function of the material used. The thermal resistance for convection and radiation paths can be calculated using the formulation:

$$R = \frac{1}{hA} \quad (12)$$

Correlations as discussed in section III are used to calculate h due to convection. The formulation below is used to calculate h due to radiation:

$$h = \varepsilon \sigma F \frac{(T_w^4 - T_\infty^4)}{(T_w - T_\infty)} \quad (13)$$

The view factor (F) has a value of 1 when a radiating surface has a perfect view of ambient. This is 0 when there is no view at all. In many cases there are convection and radiation thermal resistances in parallel.

In the steady state the temperatures at each node are calculated by solving a set of non-linear simultaneous equations of the form:

$$[1/R] \times [\Delta T] = [P] \quad (14)$$

$[1/R]$ is a square connection matrix containing conductance information. $[T]$ and $[P]$ are line matrices for the unknown nodal temperatures and known nodal power values.

For a transient calculation the thermal capacitances for each node is calculated from the specific heat capacity and weight of the relevant motor components:

$$C = \rho \times V \times C_p \quad (15)$$

The resulting set of partial differential equations are integrated using a special integration technique that gives stable solutions

in circuits having vastly different sizes of thermal capacitance – termed a stiff set of equations:

$$P = C \frac{dT}{dt} + \frac{T}{R} \quad (16)$$

$$\frac{dT}{dt} = \left[\frac{P}{C} - \frac{T}{RC} \right] \quad (17)$$

These are the types of equation that are programmed into the analytical software used in this work. The program has a sophisticated user interface to try and make thermal analysis as easy as possible to carry out by the user. To facilitate this, the user inputs the user geometry using the geometric templates shown in Figs. 4 and 5. Radial and axial cross sections are required as the heat transfer is 3-dimensional. What the motor is connected to is included in the model as it can have a significant effect on the cooling. The program automatically selects the most appropriate thermal resistance formulation for each of the nodal connections of the pre-defined network (Fig 6). The user inputs the various losses in the machine (copper, iron, friction, etc), selects materials and decides what cooling type will be modeled, i.e. TEFN, TENV, through ventilation, open end-shield, etc. The program then calculates either the steady state or transient performance as defined by the user.

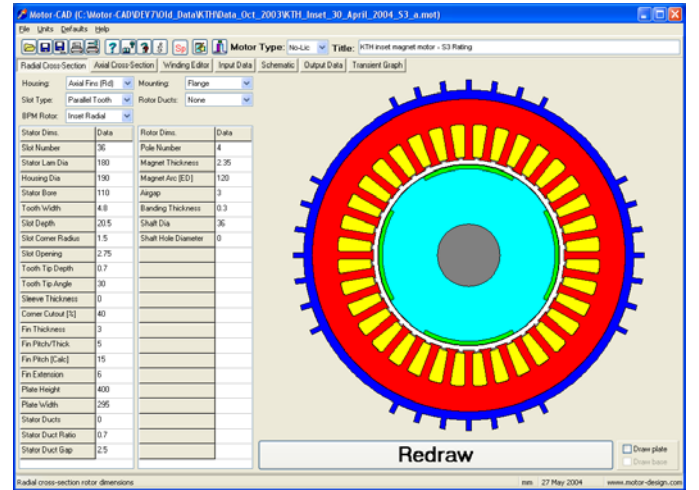


Fig. 4. Motor radial cross-section.

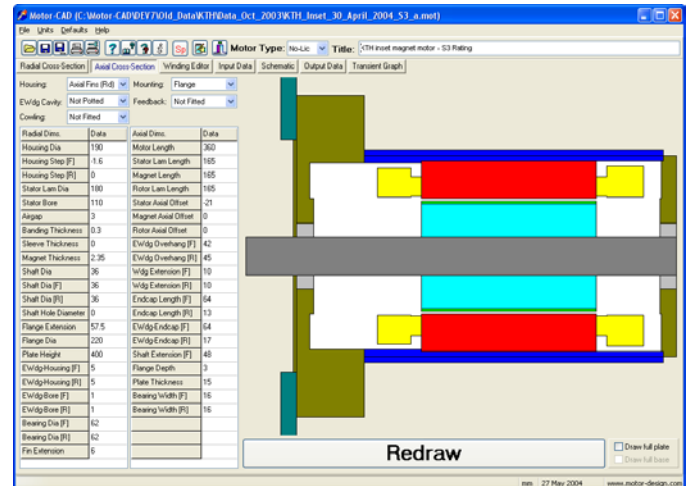


Fig. 5. Motor axial cross-section.

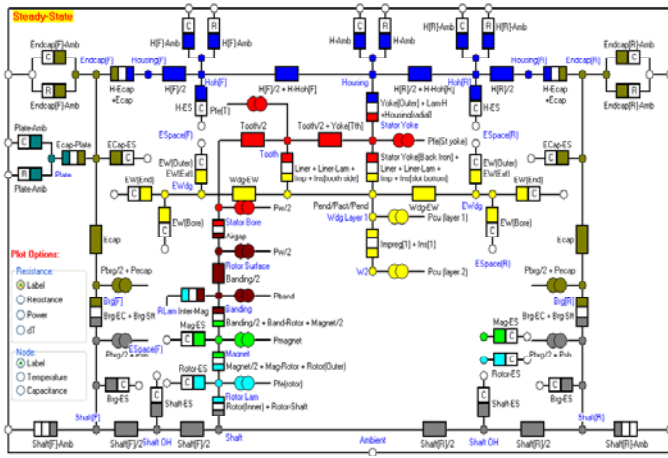


Fig. 6. Lumped-circuit model of the motor studied.

During a transient calculation it is unlikely that the losses remain constant with time. Not only may the user wish to vary the load torque (variable copper loss) and speed (variable iron loss) with time, but the winding resistance changes with the winding temperature and the magnet flux reduces slightly with the magnet temperature. There is a simple “*Loss Variation with Temperature and Load*” model built into the software to automatically account for these effects.

Several nodes are used to model the variation in temperature throughout the winding. It will tend to have a hotspot at the centre of the slot and different temperatures in the active and end winding sections. A layered winding model as depicted in Fig 7 is used to model these features. In the model we try to lump conductors together having similar temperatures. Layers of copper that have roughly equal temperature are expected to be a similar distance from the lamination to slot liner interface gap, then a slot liner (known thickness) and then layers of impregnation, wire insulation and copper. A drawing of the layered model for the motor studied here is shown in Fig 8. This schematic helps the user to visualize the slot fill (yellow copper and green insulation) and to pin point where the hot spot is likely to be. It is also useful for spotting errors in data input. It is assumed that heat transfer is through the layers thickness. The series of thermal resistances is also shown in Fig. 7. It is easy to calculate the resistance values from the layer cross-sectional area, thickness and material thermal conductivity using equation (11). For a given slot fill, when small strands of wire are selected then more conductors result. In such cases more effective gaps between conductors and thus more copper layers are expected. To achieve this the copper layer thickness is made equal to that of the copper bare diameter. The winding algorithm then iterates with the spacing between copper layers until the copper area in the model is equal to that in the actual machine. This sets the number of copper layers. The slot area left after inserting the liner and copper layers is copper insulation (enamel) and impregnation. A similar constraint is also placed on the wire insulation in that the model insulation area is equal to that in the real machine. A feature of the model is that a single impregnation goodness factor can be used to analyse the effect of air within the impregnation. It is used to form a weighted sum of impregnation and air thermal conductivity.

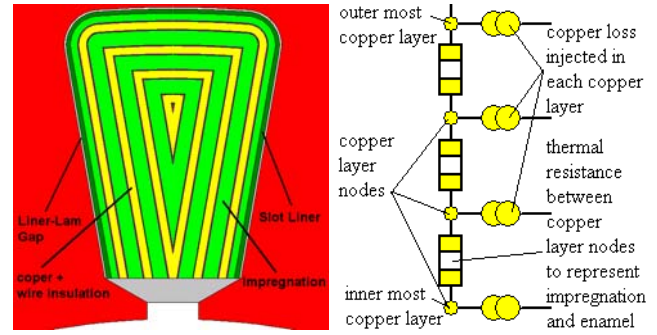


Fig. 7. Layered winding model suitable for electric machines

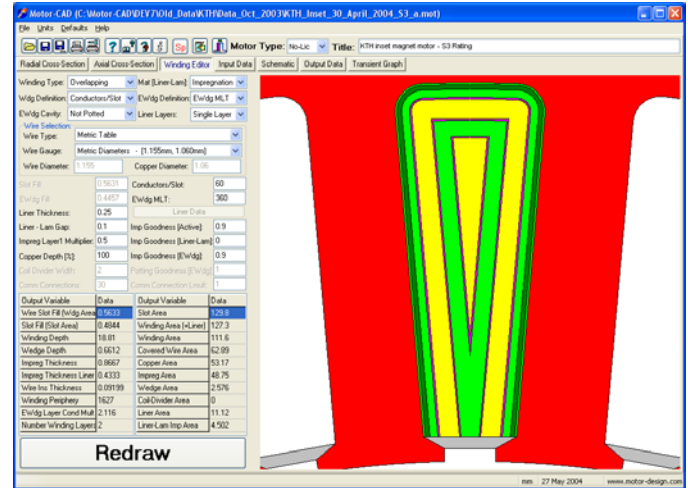


Fig. 8. Winding model for the prototype machine

V. NUMERICAL FINITE ELEMENT METHOD

It is not so common to use finite element techniques in the thermal analysis of electrical machines. This is mainly due to the fact that 3-dimensional (3-D) analysis is required to give an accurate model of the complete machine. The main advantage of the FEM approach over lumped circuit models is that a more detailed temperature resolution throughout the machines with a more complex component shapes can be gained. However, the FEM model can only give more accurate and finer details in the conducting regions of the motor as boundary conditions must be set for radiation and convection boundaries. The same analytical and empirical formulations used in the lumped circuit model are often applied here. Computational fluid dynamics (CFD) is an alternative numerical technique that is capable of modelling the convection and radiation boundaries directly. However, its complexity and computation time is an order of magnitude more than FEA, and it is not considered here.

The main disadvantage of numerical approach is the long computation times, especially when the transient analysis is required. In addition, putting together a complete model for a complex 3-D structure of the machine can also be tedious and time consuming. FEM analysis is most appropriate for the later stages of the design process to fine-tune certain geometric details. It is also advisable to just model the small section of the machine that the user is interested in gaining more detail for [1].

Two commercially available packages, FEMLAB and FLUX, have been used. Both software packages are capable of solving 2-D and 3-D problems.

A. FEMLAB

FEMLAB is an interactive environment for modelling multi-physics engineering problems based on partial differential equations (PDEs) in MATLAB. The FEM approach used to solve the PDEs. In the 3D analysis, heat transfer in a solid body is governed by the heat equation

$$\rho C \frac{\partial T}{\partial t} - \nabla \cdot (k \nabla T) = Q \quad (18)$$

where ρ is the density, C is the heat capacitance, k is the thermal conductivity and Q is the heat source. In 2D and 1D, additional transverse heat flux terms of convection and radiation are introduced to the heat source.

$$\rho C \frac{\partial T}{\partial t} - \nabla \cdot (k \nabla T) = Q + h_{trans} (T_{ext} - T) + C_{trans} (T_{ambtrans}^4 - T^4) \quad (19)$$

where h_{trans} is the convective heat transfer coefficient, C_{trans} can be defined as a radiative or emissive heat transfer coefficient, and T_{ext} and $T_{ambtrans}$ is the external and the ambient temperature respectively. In 2-D analysis, due to the symmetry of the geometry only one quarter of the machine is modelled. The boundary conditions assigned are shown in Fig. 9. The Neumann type of boundary heat flux is used for convection and radiation surfaces, i.e. the airgap and housing periphery. Values as calculated in the analytical package can be used for these boundaries.

For the 3-D analysis, only one eighth of the motor is modelled due to the symmetry. The basic geometry is obtained by extruding the main 2-D model components to their correct axial lengths (Fig. 10). End-windings are created by extending the wires bundles 30mm beyond the active region and putting additional copper between the extruding bundles. An end plate is then created to form an enclosure around the end-windings. Convective boundary conditions are assigned at the surfaces of the end-winding. Injected losses are calculated according to the volume ratio of the active to the end-winding regions.

B. FLUX

In FLUX, it is possible to parameterise the geometry, material properties and sources. Geometrical parameters such as “tooth width” and “slot depth” are used to allow the user to easily modify the construction to be modelled at solution time rather than having to make major changes in the pre-processor. It is very easy to carry out parametric studies using the software. This is useful for sensitivity analysis and optimisation.

Shell regions are used to model the thermal exchanges by radiation and convection. Heat transfer coefficient (h) values are applied to the shell region boundaries. As with FEMLAB, different values of h can be applied to the housing surface and

the airgap. Dirichlet boundary condition (fixed temperature) can also be applied if required. A limitation in 3-D is that the internal shell regions cannot be used. For this reason, the stator and rotor are modelled separately with a common airgap boundary condition. Fig. 10 shows the stator part of the 3-D geometry modelled.

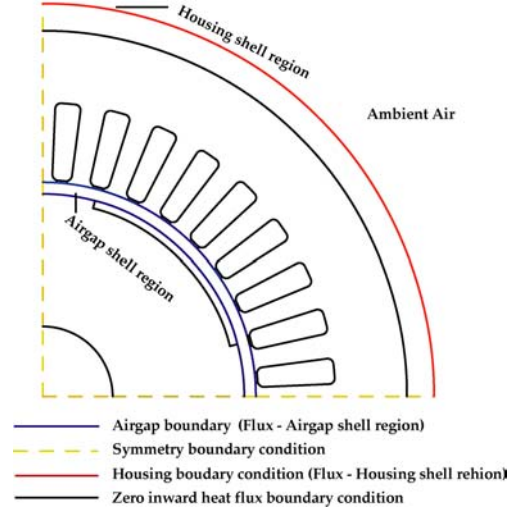


Fig. 9. 2-D geometry model and boundary conditions.

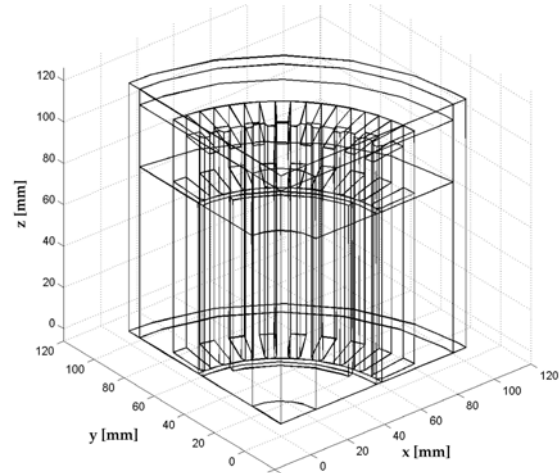


Fig. 10. 3-D geometry model used in FEMLAB.

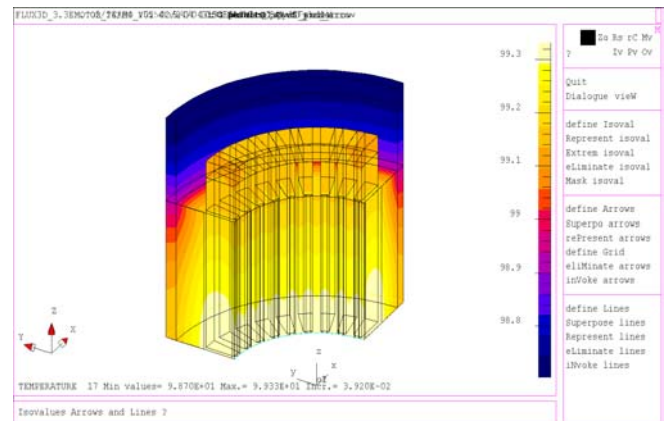


Fig. 11. 3-D geometry model applied in FLUX3D.

VI. EXPERIMENTAL MEASUREMENTS

The test bench setup is shown in Fig. 12. Five thermocouples^{1,2} are placed inside the motor, as illustrated in Fig. 13. An additional thermocouple is used to monitor the ambient temperature. Figs 14 to 16 show the experimental results measured for *S1*, *S2* and *S3* operation respectively.



Fig. 12. The test bench set up for the measurements.

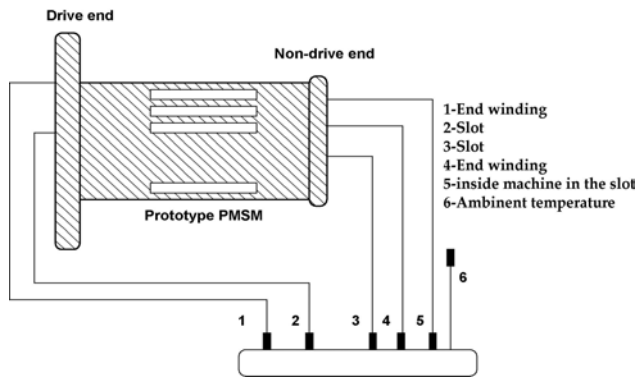


Fig. 13. Schematics of the locations of the thermocouples.

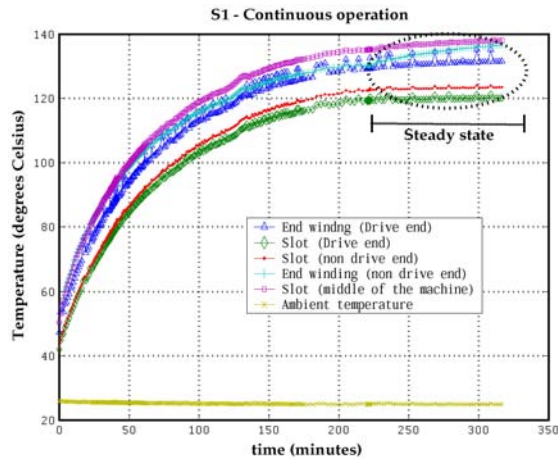


Fig. 14. S1-continuous operation at 240A.

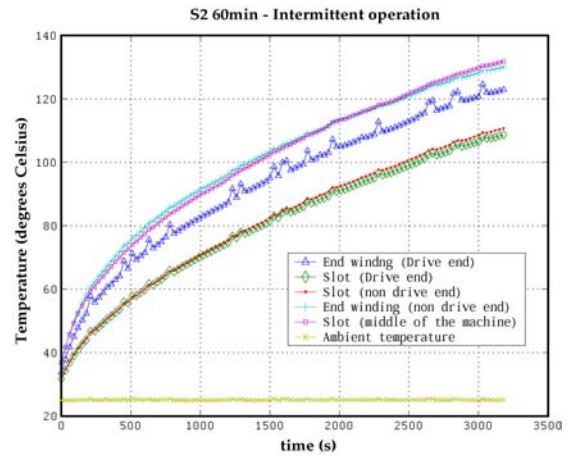


Fig. 15. S2 60min operation at 290A.

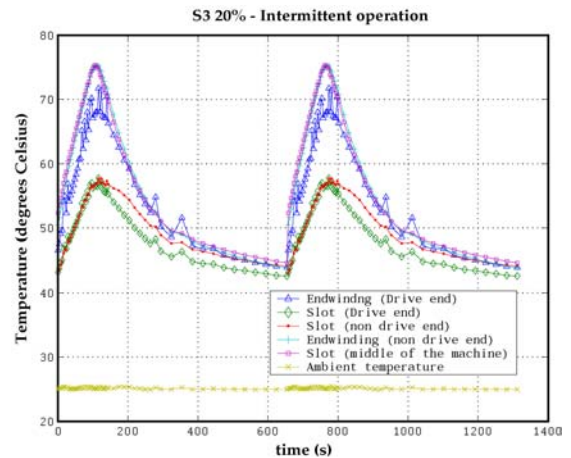


Fig. 16. S3 20% operation at 400A.

VII. RESULTS ANALYSIS

A. Lumped-circuit Analysis

A good match between the calculated and measured S1 and S2 performance is shown in Fig. 17 and 18. It is not possible to show a comparison for the loaded (heating) portion of the S3 characteristic as there were some instrumentation errors during the tests and the losses are unknown. The cooling portion of the S3 characteristic as shown in Fig. 18 shows good accuracy.

The time required to carry out these simulations is in the order of around 10 to 150 seconds on a Pentium M 1.5GHz computer. The analytical model correctly predicts that the end-windings are hotter than the active section of the winding. This is because that the end-windings are surrounded by air instead of the steel lamination, and air is an inferior heat conducting medium compared to steel. It is also noted that the non-drive temperature is slightly higher than the drive end. This is due to the cooling effect of the flange mounted test bench.

¹ Philips KTY/150 thermocouples (–40 to 300C with $\pm 5\%$ tolerance)

http://www.semiconductors.philips.com/pip/KTY84_130.html

² National Instruments, CA-1000 signal conditioning enclosure
<http://www.ni.com/pdf/products/us/2mhw263-265e.pdf>

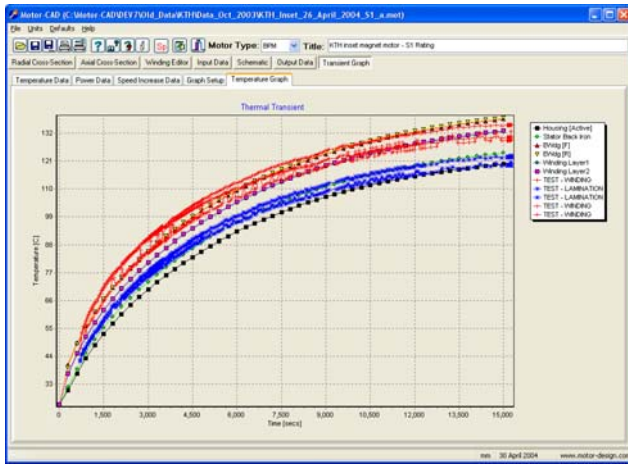


Fig. 17. S1 operation (Motor-CAD and Test).

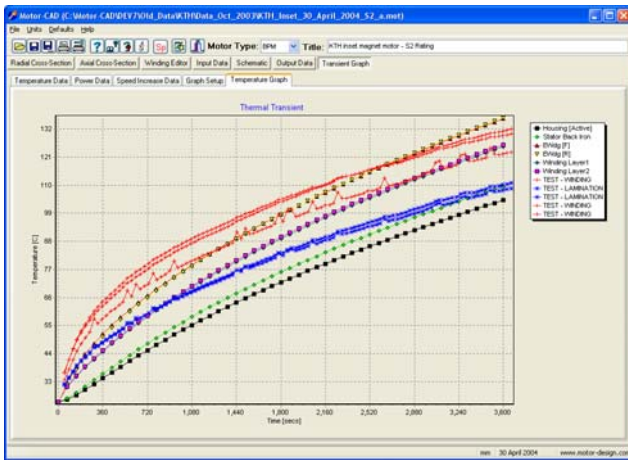


Fig. 18. S2 operation (Motor-CAD and Test).

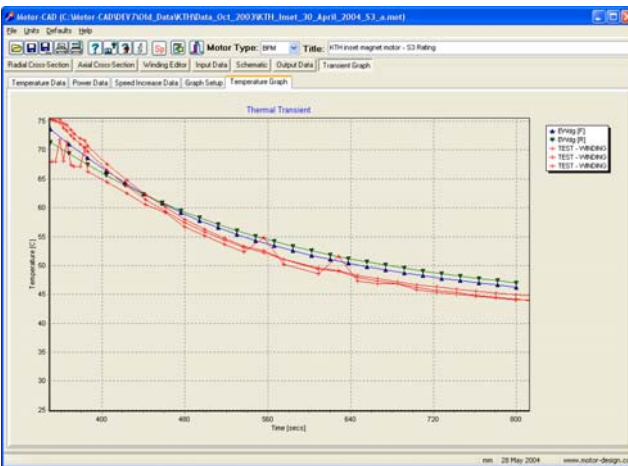


Fig. 19. S3 cooling operation (Motor-CAD and Test)

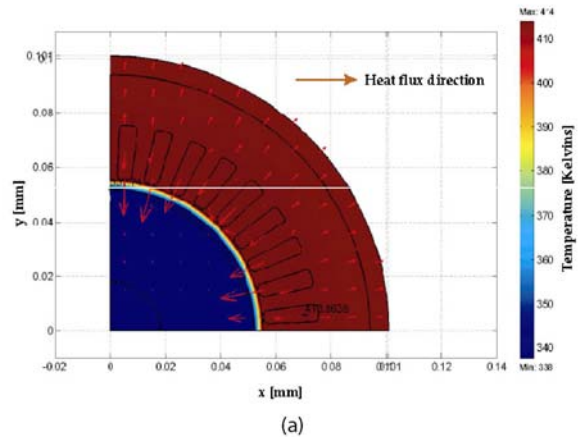
B. Numerical analysis with FEM

Finite element analysis is used to provide detail of how the temperatures vary throughout the thermally conducting regions of the machine. Fig. 11 and 20 show typical results obtained from the FEM analysis. An insight of how the temperature is distributed within the machine can be gained.

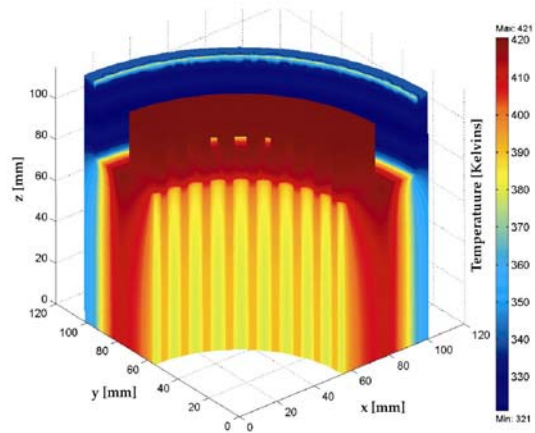
For the transient analysis very long simulation times are found. For example, just 6 time steps of the 3-D FEMLAB

model (20s step size so just 2 minutes of simulation) takes approximately three hours to solve on a *PENTIUM 4 -1.4GHZ-512 MB* computer. Eighteen hours is required on a *2.4GHZ-1GB* computer to calculate just a $15 \times 240s = 1$ hour simulation. Much less computing time is required of a 2-D numerical transient calculation, e.g. 2 hours on a *1.9GHZ-512MB* computer for a $60 \times 60s = 1$ hour simulation. Comparing to an analytical calculation, this is still many orders of magnitude slower and the model neglects many important heat transfer mechanisms.

The simulated temperature rise in the slot using FEMAB and FLUX for S1, S2 and S3 operation are compared with the measured data in Figs. 21 to 23. It can be noted that the estimated temperature rise agrees reasonably with the measurements. A similar trend of the temperature rise profile is also observed between the FEMLAB and FLUX. Discrepancies in the numerical transient calculations are mainly due to the fact that constant convection and radiation heat transfer coefficients values are applied as boundary conditions and the losses are assumed constant with time. It is much easier in the analytical model to correctly model the variation in heat transfer coefficient and losses with temperature. This further echoes that a detailed FEM simulation, especially a 3-D analysis, is more suitable to be applied at later stages of the design process for model confirmation.



(a)



(b)

Fig. 20. Temperature distribution of S1 continuous operation in: (a) 2-D; (b) 3-D analysis.

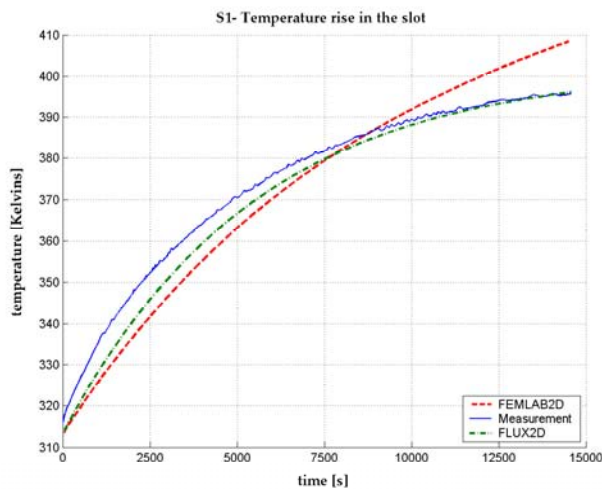


Fig. 21. The temperature rise in the slot – S1 load cycle.

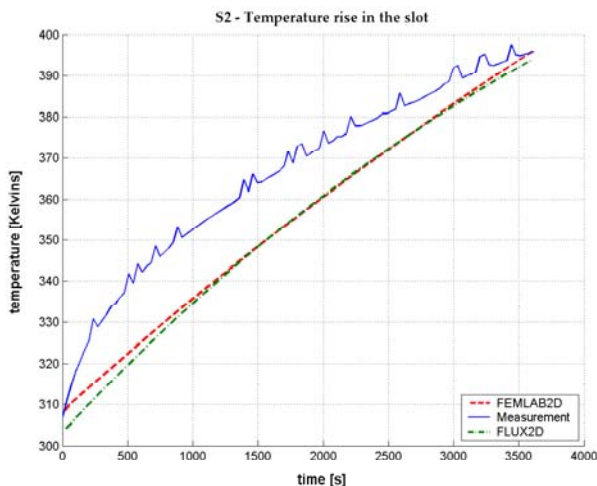


Fig. 22. The temperature rise in the slot – S2 60min load cycle.

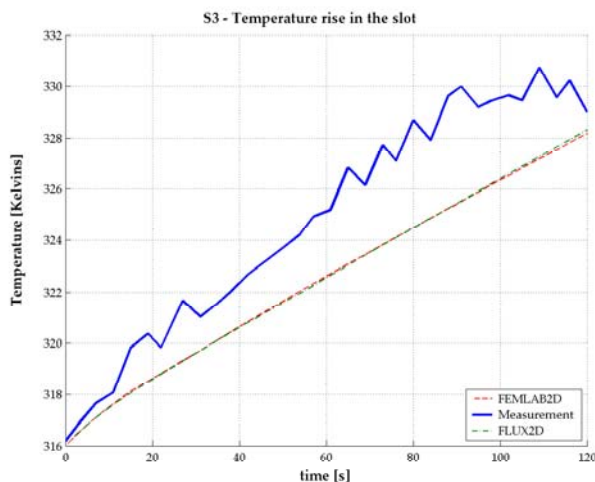


Fig. 23. The temperature rise in the slot – S3 20% load cycle.

VIII. CONCLUSIONS

The thermal analysis on a naturally cooled permanent magnet synchronous traction is presented. Both the lumped-circuit approach and the finite element method analysis are

employed in the investigations. The simulation results obtained are compared and validated by the measured data. The lumped-circuit approach has a clear advantage over the FEM analysis in terms of calculation speed, especially when carrying out transient simulations. It is also easier to model the variation in convection and radiation heat transfer coefficient with temperature in the analytical transient solution. The FEM approach do however provide a more detailed insight of the temperature variation throughout the thermally conducting regions and is more suitable for steady-state calculations at a later design stage to fine tune geometric details. Generally speaking, it is much better to use the analytical approach in the early stage of a design. A sensitivity analysis and the design optimisation can also be carried out with a relative ease.

IX. ACKNOWLEDGEMENT

The authors would like to express their gratitude to the Comsol AB for technical support in using FEMLAB, and to the Danaher Motion in Flen for providing the testing facility.

X. REFERENCES

- [1] Staton D.A, Pickering S., Lampard D., “Recent advancement in the thermal design of electric motors”, SMMA Technical Conference – Emerging Technologies for Electric Motion Industry, Oct 2001.
- [2] Staton, D.A., Boglietti, A., Cavagnino, A.: “Solving the More Difficult Aspects of Electric Motor Thermal Analysis”, IEEE IEMDC 2003 Conference Proc. 1-4 June 2003, Madison, Wisconsin, USA
- [3] Motor-CAD v1.6(42), Motor Design Ltd, www.motor-design.com
- [4] FEMLAB v2.30(b), Comsol AB.
- [5] FLUX v7.6, CEDRAT, www.cedrat.com
- [6] www.vacuumschmelze.com
- [7] Chin Y.K., Soulard J., “A permanent magnet synchronous motor for traction applications of electric vehicles”, Sixth International Power Engineering Conference (IEMDC), June 2003.
- [8] IEC standard, www.iec.ch
- [9] Boglietti, A., Cavagnino, A., Staton, D.A., “Thermal Sensitivity Analysis of TEFC Induction Motors”, IEE PEMD, April 2004
- [10] Holman J.P., *Heat Transfer*, Seventh Edition, McGraw-Hill Publication, 1992.
- [11] Taylor, G.I., “Distribution of Velocity and Temperature between Concentric Cylinders”, Proc Roy Soc, 1935, 159, PtA, pp 546-578
- [12] Mellor, P.H., Roberts, D., Turner, D.R., “Lumped parameter thermal model for electrical machines of TEFC design”, IEE Proc-B, Vol 138, No 5, Sept 1991
- [13] Schubert, E, “Heat transfer coefficients at end winding and bearing covers of enclosed asynchronous machines”, Elektrik, April 1968, Vol 22.
- [14] DiGerlando, A., Vistoili, I., “Thermal Networks of Induction Motors for Steady State and Transient Operation Analysis”, ICEM 1994, Paris.
- [15] Stokum, G, “Use of the results of the four-heat run method of induction motors for determining thermal resistance, Elektrotechnika”, 1969, Vol 62, No 6.
- [16] Hamdi, E.S., *Design of Small Electrical Machines*, Wiley, 1994.
- [17] Chin Y.K., Nordlund E., Staton E.A., “Thermal analysis – Lumped circuit model and finite element analysis”, Sixth International Power Engineering Conference (IPEC), pp. 952-957, Nov 2003.